Journal of Marine Systems 179 (2018) 72–87

Contents lists available at ScienceDirect

Journal of Marine Systems

journal homepage: www.elsevier.com/locate/jmarsys

Links between phytoplankton dynamics and shell growth of *Arctica islandica* on the Faroe Shelf

Fabian Georg Wulf Bonitz[a,*], Carin Andersson[a], Tamara Trofimova[a], Hjálmar Hátún[b]

[a] Uni Research Climate, Bjerknes Centre for Climate Research, Bergen, Norway
[b] Faroe Marine Research Institute, Box 3051, FO-110 Tórshavn, Faroe Islands

ARTICLE INFO

Keywords:
Arctica islandica
Shell growth
Phytoplankton dynamics
Faroe Shelf

ABSTRACT

The phytoplankton dynamics on the Faroe Shelf are strongly connected to higher trophic levels, and their inter-annual variability has great importance for many organisms, including the principal fish stocks. Hence, information on the marked phytoplankton variability is scientifically and economically valuable. We show here that the shell growth variability in *Arctica islandica* shells has the potential to identify periods of increased and decreased phytoplankton concentrations on the Faroe Shelf and in the wider Faroese region in previous centuries. The growth of *A. islandica* has often been linked to changes in phytoplankton concentrations, i.e., food availability. By cross-matching life-collected and sub-fossil *A. islandica* shells from two separate locations on the Faroe Shelf, we have built a master chronology, which reaches back to the 17th century. This master chronology correlates well with a Primary Production index for the Faroe Shelf ($r = 0.65$; $p < 0.01$) and average April–June chlorophyll *a* concentrations in the central part of the shelf ($r = 0.74$; $p < 0.01$). A link is also identified between the shell growth and phytoplankton concentrations over the wider Faroese Channel Region, as represented in the Continuous Plankton Recorder surveys, especially for the months June–September ($r = 0.39$; $p < 0.01$). In addition, an inverse relationship is observed between the master chronology and on-shelf water temperatures from June–September ($r = -0.29$; $p < 0.01$), which is likely associated with a previously reported inverse relationship between temperatures and the on-shelf primary production. An analysis of the $\delta^{18}O$ in the shells shows that the main growing season of the shells presumably occurs during the spring and summer months, which concurs with the main spring bloom.

1. Introduction

Primary production and its annual and inter-annual variability on the Faroe Shelf (Fig. 1) have been the focus of many studies (e.g., Debes et al., 2008; Eliasen et al., 2017a; Gaard et al., 1998; Hansen et al., 2005). In this area and in the wider Faroese region, primary production is strongly connected to higher trophic levels (Gaard et al., 2002; Hátún et al., 2009). Generally, the Faroe Shelf has a rich and diverse ecosystem (Homrum et al., 2012; Steingrund and Gaard, 2005) and is of great importance as a nursing ground for various economically important fish stocks (Gaard et al., 2002). Hence, a better understanding of phytoplankton dynamics through time is valuable. Systematic instrumental observations including phytoplankton dynamics, water temperatures and salinities have mainly been carried out since 1988 with the establishment of the Faroese Standard Sections (Larsen et al., 2012). On-shelf primary production data are particularly limited before that time. Thus, understanding of the long-term phytoplankton dynamics on the Faroe Shelf is also limited.

The shell growth of the mollusc species *Arctica islandica* (Linnaeus, 1767) (Fig. 2) has often been related to environmental and climatic variables such as food availability (Witbaard et al., 1997a) or water temperature (e.g. Butler et al., 2010; Marali and Schöne, 2015) and has been found to be strongly influenced by these two parameters (Ballesta-Artero et al., 2017; Schöne et al., 2005a; Witbaard et al., 1997a). In general, *A. islandica* has been proven to be a good tool in paleoclimate reconstructions for the Holocene (Schöne, 2013) and has been used in a variety of paleoclimate studies (e.g. Butler et al., 2011; Schöne et al., 2005b; Wanamaker et al., 2011). Specimens of *A. islandica* can be found across the North Atlantic to water depths of over 500 m (Nicol, 1951) and can be exceptionally long-lived with a maximum recorded age of 507 years (Butler et al., 2013). A key aspect of *A. islandica* is the formation of annual growth increments in its shell (Jones, 1980; Schöne et al., 2005a) and the fact that the variation in width of the growth increments can be related to environmental and climatic changes (Witbaard et al., 1997a). The width of the growth increments is defined by annual growth lines (Jones, 1980), which form due to drastically

* Corresponding author at: Uni Research Climate, Jahnebakken 5, 5007 Bergen, Norway.
E-mail address: fabian.bonitz@uni.no (F.G.W. Bonitz).

https://doi.org/10.1016/j.jmarsys.2017.11.005
Received 9 June 2017; Received in revised form 21 November 2017; Accepted 29 November 2017
Available online 02 December 2017

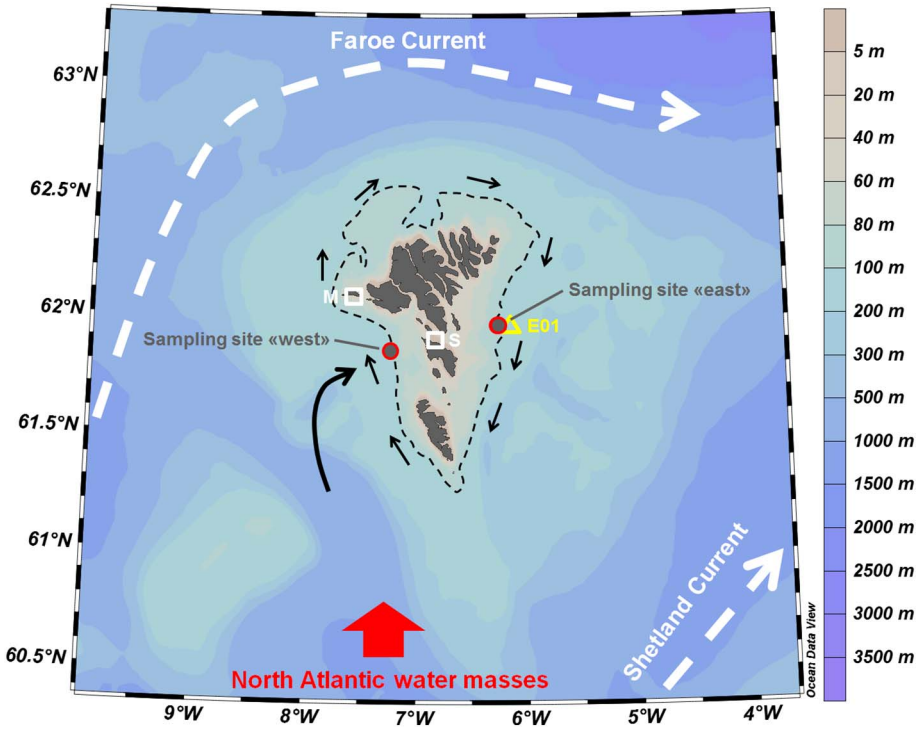

Fig. 1. Faroe Shelf with the sampling locations (red circles) and the main oceanographic features. The black dashed line is the 100 m depth contour, and the thin black arrows indicate the flow direction of the on-shelf water masses. The thick black arrow indicates the main inflow path of off-shelf water masses onto the Faroe Shelf. The white squares represent the coastal monitoring stations Skopun (S) and Mykines (M), and the yellow triangle represents the CTD station E01, which is part of the Faroese Standard Sections. (For interpretation of the references to color in this figure legend, the reader is referred to the web version of this article.)

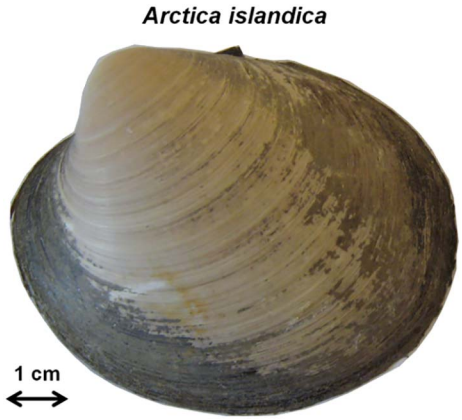

Fig. 2. Left valve of an *A. islandica* shell from the Faroe Shelf.

reduced growth rates during a certain time of the year (Dunca et al., 2009). The application of cross-dating techniques from dendrochronology and the stacking of temporally aligned specimens of *A. islandica,* also referred to as time series, can be used to construct shell-based master chronologies, which reflect the growth increment variability among several specimens from a population (e.g. Butler et al., 2010; Marchitto et al., 2000) and provide annually resolved and precisely dated paleorecords (e.g. Scourse et al., 2012; Weidman et al., 1994). The growth increment variability expressed by a master chronology is referred to in this study as "shell growth variability". Especially over the last two decades, several of these shell-based chronologies have been constructed in the North Atlantic realm (e.g. Butler et al., 2013; Mette et al., 2016). The shells of *A. islandica* also incorporate various geochemical signals (e.g. Schöne et al., 2011; Weidman and Jones, 1993). For example, the common technique of using $\delta^{18}O/\delta^{16}O$ ratios in paleoclimate studies for temperature reconstructions has been reliably performed on shells of *A. islandica* (e.g. Reynolds et al., 2016; Schöne et al., 2005b). When applying molluscan sclerochronology on the species *A. islandica*, detailed knowledge about the environmental and climatic conditions of the study area is essential because the actual response of the shell growth to changes in food availability and water temperatures varies between different locations (Schöne, 2013).

Here, the Faroe Shelf is considered to be a good location for sclerochronological studies since the central part of the on-shelf water masses is fairly homogenous, both vertically and horizontally, throughout most of the year (Larsen et al., 2008), local primary production shows strong intra-annual and inter-annual variability (Gaard, 2003), and the instrumental coverage for comparisons is extensive. Further advantages of the Faroe Shelf are the abundant presence of *A. islandica* and good accessibility to *A. islandica* specimens in this area.

The main focus of this study is to test whether the shell growth variability can serve as a tool for estimating past year-to-year and potential long-term phytoplankton dynamics by examining how well variations in phytoplankton concentrations in the Faroe Shelf and in a broader spatial context are captured in the growth increment variability of the shells of *A. islandica*.

2. Area of investigation

The Faroe Shelf is encompassed by the relatively warm water masses of two branches derived from the North Atlantic Current (Hansen and Østerhus, 2000): the Faroe Current to the north and the Shetland Current to the south of the Faroe Islands (Hansen et al., 2003). Off-shelf water masses are brought onto the Faroe Shelf mainly from the west (Larsen et al., 2009). However, tidal rectification on the Faroe Shelf leads to a clockwise current around the Faroe Islands (Fig. 1) (Hansen, 1992; Larsen et al., 2008), leaving the Faroe Shelf partially isolated from off-shelf water masses (Larsen, 2003; Larsen et al., 2009). The Faroe Shelf can be divided into an inner (Central) and Outer shelf, which have different densities due to temperature and salinity differences (Eliasen et al., 2017a). The Central shelf covers the area within a 100 m depth contour, and the Outer shelf roughly corresponds to an area between the 100 m and 160 m depth contours (Larsen et al., 2008). The Outer shelf experiences seasonal stratification, especially during the summer/fall months (Larsen et al., 2009). In contrast, the water masses from the Central shelf are fairly homogenous and vertically well-mixed throughout the year (Larsen et al., 2008).

The setting and the special characteristics of the Faroe Shelf strongly influence phytoplankton dynamics and primary production in this area (Debes et al., 2008; Hansen et al., 2005). Overall, the on-shelf primary production shows strong intra-annual and inter-annual variability (Gaard, 2003), and its controlling mechanisms have been intensively debated (e.g. Debes et al., 2008; Eliasen et al., 2016; Gaard et al., 1998; Hansen et al., 2005). The controlling mechanisms behind the variability of primary production on the inner part of the Faroe Shelf is likely linked to the intensity of exchange rates between the Central shelf and the Outer/off shelf water masses during the spring months (Debes et al., 2008; Eliasen et al., 2005; Eliasen et al., 2016; Hansen et al., 2005) and nutrient renewal from the Outer/off shelf during the summer and fall months through "ocean-to-shelf nutrient fluxes" (Eliasen et al., 2016; Eliasen et al., 2017b). This nutrient import is, in turn, likely controlled by large-scale primary production drivers operating in a broader spatial context (Eliasen et al., 2017a; Hátún et al., 2009). One example of this is the similarity between phytoplankton concentration patterns from the Outer shelf and patterns, which can be observed on the European margin (Eliasen et al., 2017a).

3. Material and methods

3.1. Sampling

The shell material was collected from the Faroe Shelf during the MH1422 and GS14 cruises in 2014. The first cruise took place in June 2014 onboard the Faroese research vessel *Magnus Heinason,* and the second cruise in November 2014 was onboard the Norwegian research vessel *G.O. Sars*. The shells were recovered from the sea floor by dredging. Shells were collected from several stations on the eastern and western sides of the Faroe Islands from water depths between 90 and 120 m. This also means that the shells were collected at the border of the Central and Outer shelf.

3.2. Growth increment analysis

Acetate peels were prepared from the shell cross-sections to make the growth lines more visible and easier to work with. A detailed description of the shell processing can be found in Butler et al. (2009b) and Scourse et al. (2006). The acetate peels were investigated under a Nikon Eclipse ME600L light microscope with magnifications of × 25, × 50 and × 100, depending on the area of interest, using transmitted light and were photographed with a Lumenera Infinity 3 camera. The growth increment analysis was done using the image processing software Image-Pro Premier. All measurements of the growth increments were performed along the margin of the shell. The identification of single growth increments is based on the study by Butler et al. (2009a).

3.3. Cross-dating

To obtain a robust start for an annually-resolved chronology, the growth-increment series of live-collected specimens were cross-dated first since the year of death (2014) of these specimens is known. Cross-dating describes the process of visually matching temporally overlapping time series based on synchronous growth increment patterns induced by a common external driver. This enables the identification of any dating errors (e.g. missing or false increments) and allows growth increments to be brought into exact temporal alignment. For more information on cross-dating see Speer (2010) and Baillie (1982). After a robust start for the chronology had been established, time series of articulate sub-fossil and single-valve subfossil specimens were cross-dated against the live-collected specimens thereby extending the chronology farther back in time. The visual cross-dating process was based on the identification and investigation of so-called "marker years" and the use of skeleton plots. Marker years are growth increments, which are either very narrow or wide in comparison to their adjacent growth increments. For the subsequent statistical evaluation of cross-dating, the programs SHELLCORR (Scourse et al., 2006) and COFECHA were used.

3.4. Chronology construction

The master chronology was developed by including 34 specimens from the eastern sampling site and 5 specimens from the western sampling site. First, the measurements of each times series were detrended with a negative exponential function to remove age-related growth trends, and in the process, the variance of the increment width was stabilized by using an adaptive power transformation. The predicted values from the detrending process were divided by the observed values and thereby standardized to a mean of one. For the final construction of the chronology, the detrended measurements of the time series were averaged with a biweight robust mean. The assessment of the quality of the chronology was based on the Expressed Population Signal (EPS), which quantifies the extent to which the common environmental signal in a population is expressed in the chronology. Here, a value equal to or above 0.85 is considered sufficient, as suggested by Wigley et al. (1984). The EPS was calculated in a 30-year window with an overlap of 29 years. All mathematical operations mentioned above were carried out using the software ARSTAN (Cook and Holmes, 1986).

Due to rapid growth in the ontogenetically young part of the shell, it is not possible to perform measurements of widths perpendicular to the growth lines. Growth increment measurements in this part of the margin are only possible at a much smaller angle in relation to the growth lines (Schöne, 2013), which would result in an overestimation of the growth. In general, in *A. islandica,* this occurs in the first 40 growth increments (Schöne, 2013). In this study, the number of years that cannot be measured perpendicularly vary between specimens, but on average, the first 10 growth increments were affected. These growth increments were not considered in the chronology construction process but were still brought into an exact temporal context because of the $\delta^{18}O$ analyses (Section 3.5).

3.5. $\delta^{18}O$ analysis

The $\delta^{18}O$ record of single growth increments in the shells of *A. islandica* can capture seasonal temperature cycles (Schöne et al., 2005c). Thus, an oxygen isotope analysis was performed on selected shells to establish the growing season of *A. islandica* on the Faroe Shelf. For the oxygen isotope analysis, samples were taken by drilling from the cut surface of the cross sections of specimens from the eastern shell collection site. The holes were drilled along the outer margin of a specimen with a 0.3 mm-wide drill bit (Komet/Gebr. Brasseler GmbH and Co. model no. H52 104 003) attached to a Minimo One Series Vers. 2 drilling device. The powder samples were sent to the Institute of Geoscience at the Johannes Gutenberg University (JGU) in Mainz, Germany for the geochemical analyses. The samples were analyzed using a Finnigan MAT 253 continuous-flow mass spectrometer equipped with a Gas-Bench II. The long-term external precision (1σ) of the mass spectrometer measurements was better than ± 0.06‰ for $\delta^{18}O$, based on blind measurements of NBS-19 calibrated in-house standard Carrara-Marble (− 1.91‰). The $\delta^{18}O$ measurements of the samples are reported relative to Vienna Peedee Belemnite (VPDB).

To reconstruct the seasonal isotope signal in single growth increments, samples were drilled in relatively wide growth increments of ontogenetically young specimens. To compare the seasonal signals in the $\delta^{18}O$ compositions of the shells with instrumental data, growth increments, which reflect recent calendar years, were selected since the instrumental coverage is better for these years. Additionally, the wide increments in the young shell portion of ontogenetically older specimens were also used in $\delta^{18}O$ analyses. The number of samples taken per growth increment depends on the width of the growth increment but varied between 3 and 19 per increment. The depth of a single hole was

kept as shallow as possible but was deep enough to obtain a sample size of between 40 and 120 µg, which is required for the stable isotope analysis in the mass spectrometer.

To transform the shell $\delta^{18}O$ values to temperature, the paleothermometry equation by Grossman and Ku (1986) was used (Eq. (1)). Since Grossman and Ku (1986) reported $\delta^{18}O_{water}$ values against SMOW-0.27‰, a modification of the equation (− 0.27) was applied, as further explained by Sharp (2007).

$$\text{Temperature } \delta^{18}O\ (^{\circ}C) = 20.6–4.34\cdot(\delta^{18}O_{shell}-(\delta^{18}O_{water}-0.27)) \quad (1)$$

The value for the $\delta^{18}O_{water}$ used in the equation was obtained from bottom water samples, which were collected close to the shell collection site on the eastern side of the Faroe Islands. The water samples were collected during the GS14 cruise in November 2014, and additional water samples were collected in February 2017 onboard the research vessel *Magnus Heinason*. The water samples from the GS14 cruise in 2014 were analyzed at the Institute of Geoscience at the JGU in Mainz, Germany and at the Department of Earth Science at the University of Bergen, Norway. The water samples from February 2017 were only analyzed at the Department of Earth Science at the University of Bergen, Norway. For the $\delta^{18}O_{water}$ analysis in Mainz, the international standards GISP2 (− 24.76‰), VSMOW2 (0‰), and SLAB2 (− 55.5‰) were used. For the $\delta^{18}O_{water}$ analysis in Bergen, the in-house standards DI (− 7.71‰), SeaII (0.25‰), EVAP (5.03‰), and sea old (0.89‰) were used, which had been calibrated against the international standards GISP, VSMOW2, and SLAB2. The results are reported relative to Vienna Standard Mean Ocean Water (V-SMOV).

3.6. Instrumental data

To reveal the potential relationships between the shell growth and phytoplankton dynamics, the master chronology is compared to a variety of phytoplankton datasets from the Faroe Shelf and the wider Faroese region. Generally, monthly averages were used. On the Faroe Shelf, chlorophyll *a* concentrations are related to primary production (Eliasen et al., 2011). Thus, the integrated chlorophyll *a* concentrations from April to late June from the coastal monitoring station Skopun (Fig. 1) on the Faroe Shelf were used (see Eliasen et al., 2011). The chlorophyll *a* concentrations have been measured spectrophotometrically on a weekly basis since 1997. In addition, satellite chlorophyll *a* measurements (see Maritorena et al., 2002) were used. The data were downloaded from the GlobColour Project homepage (www.globcolour.info, last accessed June 2017) and represents near-surface chlorophyll *a* concentrations from 1998 to 2013. The grid

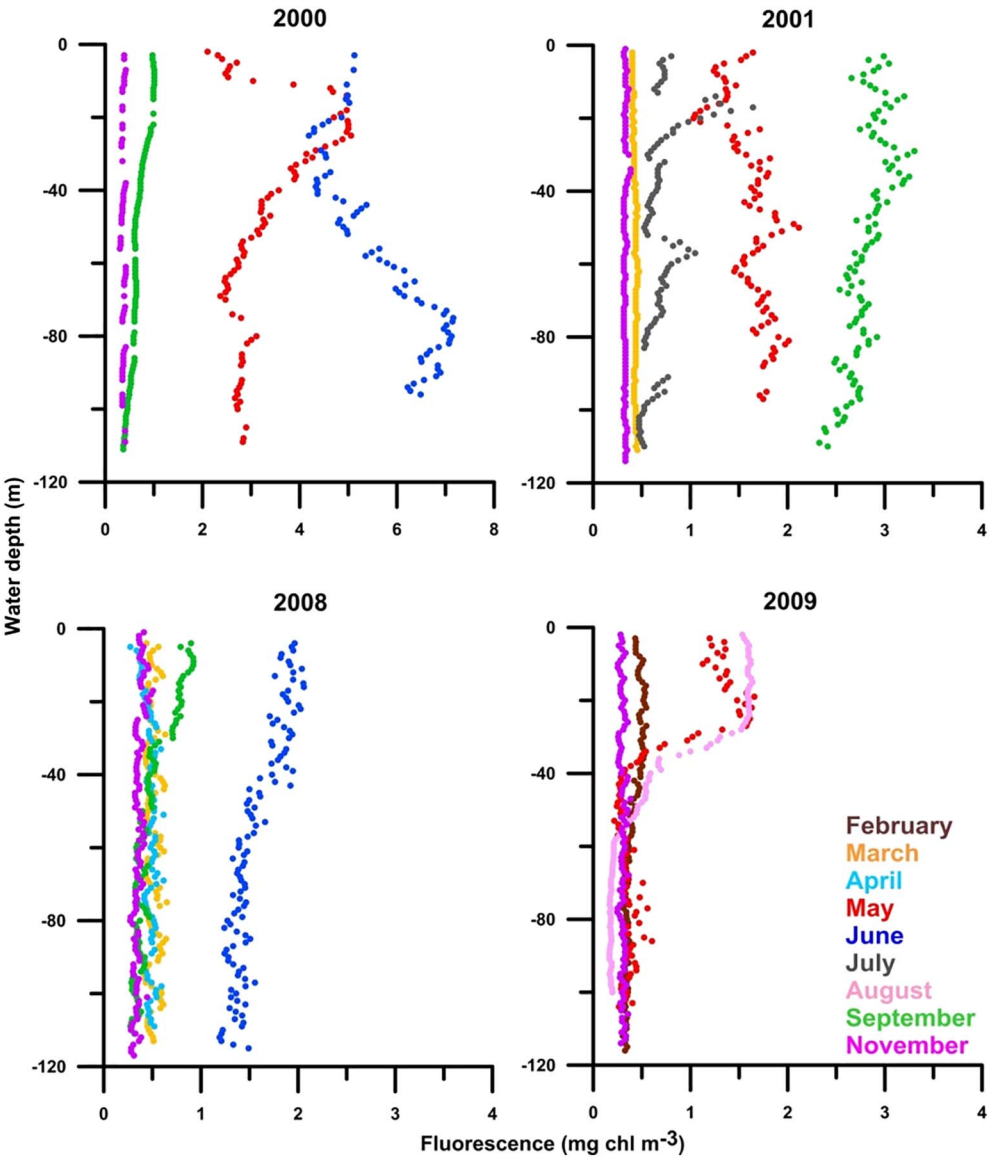

Fig. 3. Fluorescence profiles from the CTD station E01 in various months in the years 2000, 2001, 2008, and 2009. (For interpretation of the references to color in this figure legend, the reader is referred to the web version of this article.)

resolution is 4 km, and the satellite chlorophyll *a* measurements were extracted for the area covering the Faroe Shelf (60–64°N, 3–10°W). Additionally, a Primary Production index (PP-index) (Gaard, 2003; Gaard et al., 2002) from the Faroe Shelf was used. The PP-index is calculated from the on-shelf nitrate reduction from winter to late June. It mainly reflects the "accumulated new primary production in the Faroe shelf water ecosystem during spring and summer" (Eliasen et al., 2011). Higher PP-index values reflect increased primary production and vice versa. On-shelf fluorescence profiles (Fig. 3), which allow estimations of phytoplankton concentrations, were obtained from a standard Conductivity, Temperature, Depth (CTD) station (E01), which is located close to the shell collection site on the eastern side of the Faroe Shelf (Fig. 1). The CTD casts have not been consistently made on the same months/days of the different years and have not been repeated either within a certain month. Thus, the CTD measurements of single months represent snapshots and may not robustly reflect the average conditions of a given month. The months with the most available data are February, May, September, and November. Phytoplankton data from the wider Faroese region are derived from the Continuous Plankton Recorder (CPR) survey (Batten et al., 2003). The CPR dataset used in this study (doi: https://doi.org/10.7487/2017.47.1.1033) consists of monthly phytoplankton concentrations and an annual Phytoplankton Color Index (PCI) for the period 1958–2016, covering the wider Faroese Channel Region and representing the 0–10 m water column. The PCI is based on the visual analysis of the phytoplankton pigments in a CPR sample, using spectrophotometric methods and is a semi-quantitative representation of the total phytoplankton biomass.

To test the effect of temperature on the shell growth, the master chronology was also compared to temperature data from the Faroe Shelf. These data were further used to define the main growing season more precisely by comparing the $\delta^{18}O_{shell}$-based temperature reconstructions with the instrumental temperature data. The water temperatures from the Central shelf span the periods from 1914 to 1968 and 1992–present. The water temperatures from 1914 to 1968 are drawn mainly from daily measurements at a coastal station on Mykines on the western side of the Faroe Islands (Fig. 1). The water temperatures for the period from 1992 until today have been collected at the coastal monitoring station in Skopun. Since instrumental observations from the Central shelf have shown that the water temperatures are horizontally and vertically very similar to approximately 100 m (Larsen et al., 2008), we assume that the measured water temperatures in Mykines and Skopun also reflect the water temperatures conditions in the sampling areas. Since air and water temperatures on the Faroe Shelf are strongly coupled, the master chronology was also compared to monthly air temperatures from the Faroe Islands. The air temperature data were drawn from the "6011 THORSHAVN" (World Meteorological Organization station code) weather station in Torshavn. The air temperatures there have been measured since 1867 with an interruption from 1925 to 1930. The average monthly air temperature data from this station were downloaded from the Koninklijk Nederlands Meteorologisch Instituut (KNMI) database (www.knmi.com, last accessed March 2017). The annual averages of the water temperature dataset and the air temperature dataset correlate well ($r = 0.8$; $p < 0.01$).

3.7. Statistics

For comparisons between the master chronology and phytoplankton and temperature datasets, the Pearson correlation was used and, in some cases, the Spearman rho correlation. The commonly used p value of 0.05 was chosen as the threshold value for correlations to be considered significant. To evaluate the combined effect of phytoplankton dynamics and temperatures on the shell growth, a stepwise multiple regression was applied. The results of the regression analysis are given as adjusted R^2 values.

4. Results

4.1. Chronology

The shell-based growth record covers the time period from 1625 to 2013 and consists of 9 live-collected, 12 articulate sub-fossil and 18 single-valve sub-fossil specimens (Fig. 4). The chronology, here defined as part of the shell-based growth record, which shows EPS values higher than 0.85, covers the time period from 1663 to 2013. The overall series intercorrelation is 0.78 and there are no differences in cross-dating across the two sampling locations, meaning that the growth increment patterns in the specimens from the eastern and western sampling location are synchronous. The average correlation of the series in 30-years segments lagged by 15 years is always equal to or above 0.67. The correlation between the single time series and the master series is always higher than 0.50 with the exception of one time series, which only shows a correlation of 0.32 with the master series. Four times series

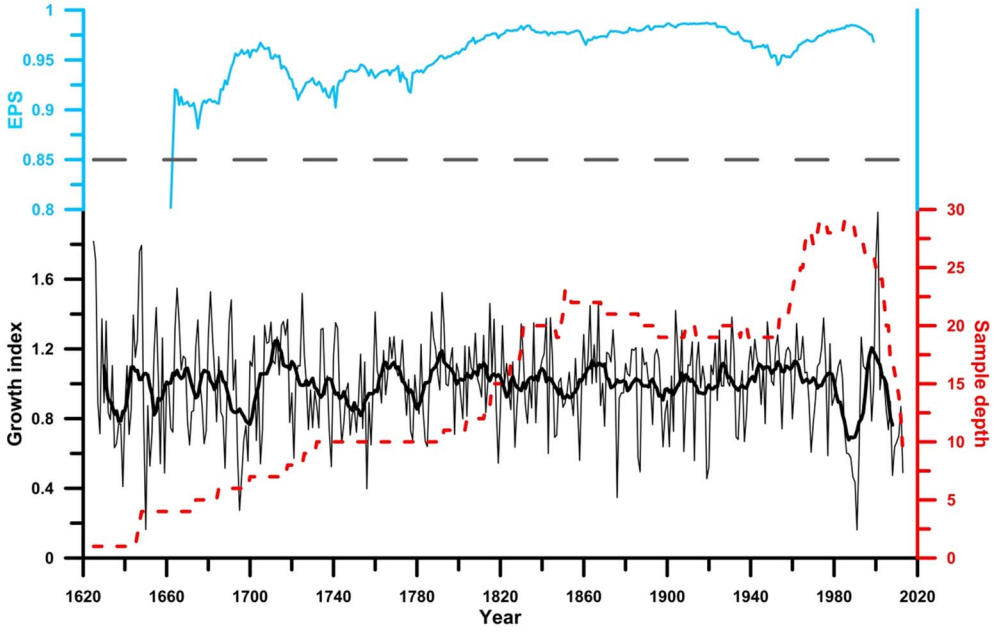

Fig. 4. Growth index of the master chronology (thin black line) and the 11-year running mean (thick black line). The red dashed line represents the sample depth, and the light blue line represents the Expressed Population Signal (EPS) as calculated in a 30-year window. The gray dashed lines indicate the EPS threshold value, above which the chronology is statistically robust. (For interpretation of the references to color in this figure legend, the reader is referred to the web version of this article.)

show higher correlations in certain segments at other-than-dated positions, suggesting potential dating errors. A detailed visual investigation of these time series in the respective segments could not confirm the dating errors. Hence, we assume that the cross-dating of these time series is correct and that the suggested higher correlations at the other-than-dated positions are spurious. A detailed overview of the statistical cross-dating is provided in Appendix A.

4.2. $\delta^{18}O$ results and growing season

The $\delta^{18}O_{shell}$ values cover a range of up to 0.8‰ in single growth increments and tend to be highest during the youngest part of a growth increment and lowest during the oldest part of a growth increment (Fig. 5). The maximum range of all measurements is 1.44‰.

The analysis of the 2014 water samples at the two different laboratory facilities resulted in different $\delta^{18}O_{water}$ values. The $\delta^{18}O_{water}$ value of the samples measured at the Institute of Geoscience at the JGU in Mainz is 0.85‰ for the first run and 0.6‰ for the second run. The $\delta^{18}O_{water}$ value of the 2014 samples measured at the Department of Earth Science, University of Bergen is 0.4‰. The $\delta^{18}O_{water}$ value of the 2017 samples measured at the Department of Earth Science, University of Bergen is 0.27‰. When using the four different values of the measured $\delta^{18}O_{water}$ (0.85‰, 0.6‰, 0.4‰, and 0.27‰) in the Grossman and Ku (1986) equation, the shell-based reconstructed water temperatures (minimum and maximum) vary between 10.28 °C and 16.52 °C for $\delta^{18}O_{water}$ = 0.85‰, between 9.20 °C and 15.44 °C for $\delta^{18}O_{water}$ = 0.6‰, between 8.33 °C and 14.57 °C for $\delta^{18}O_{water}$ = 0.4‰, and between 7.75 °C and 14.00 °C for $\delta^{18}O_{water}$ = 0.27‰. In general, the reconstructed temperatures are 2.9°-5.5 °C (depending on the utilized $\delta^{18}O_{water}$ value) higher and barely overlap with instrumental measurements at any time of the year (Fig. 6). In addition, some of the reconstructed temperatures approach (and even reach) lethal temperatures for the species *A. islandica* at approximately 16 °C (e.g. Mann, 1989). Given that the bottom water temperature at the sampling sites during the summer months can sometimes be colder than the SST by approximately 1 °C, the offset between the reconstructed and actual temperatures is even larger. To match the reconstructed temperatures from single growth increments with the observed seasonal temperatures, a $\delta^{18}O_{water}$ value of − 0.43‰ would be required (Fig. 6). Seawater $\delta^{18}O$ values can also be estimated from measured salinity using a mixing line, which covers the water masses of the area of interest. Based on the average salinity value of 35.1‰ (derived from the CTD station) in bottom waters at the shell location, the North Atlantic mixing line (Craig and Gordon, 1965) and

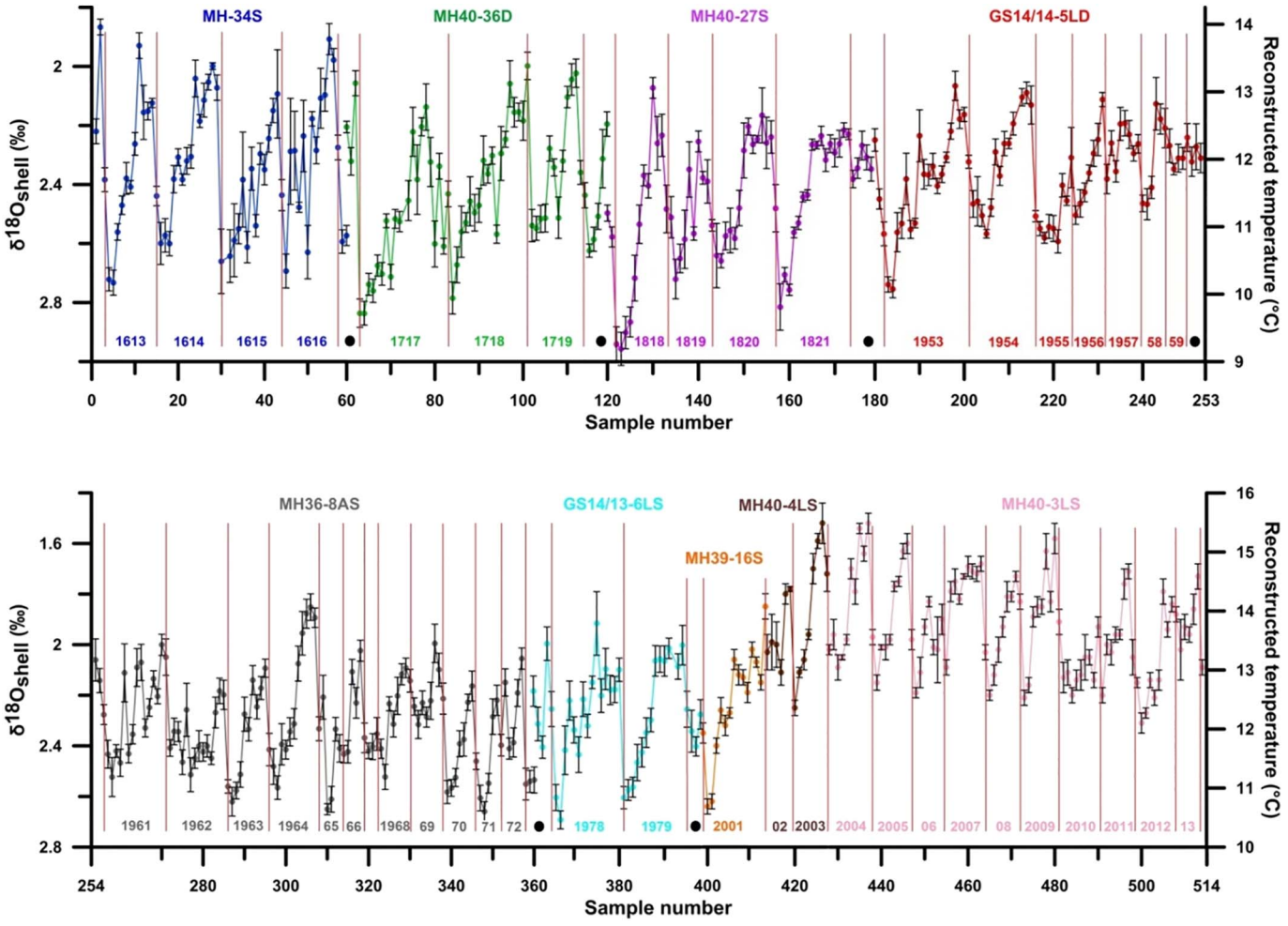

Fig. 5. Measured $\delta^{18}O_{shell}$ values and reconstructed temperatures using a $\delta^{18}O_{water}$ value of 0.6‰ in the Grossman and Ku (1986) equation. The period from 1953 to 1980 does not include $\delta^{18}O_{shell}$ values from 1974 to 1976 due to the lack of appropriately wide growth increments in this period. The black bars represent the replicated precision which is a calculation of how much the $\delta^{18}O_{shell}$ values of a single sample vary for repeated (here 8 times) $\delta^{18}O$ measurements in the mass spectrometer. The $\delta^{18}O_{shell}$ values are derived from several specimens. The specimen code can be found above the $\delta^{18}O_{shell}$ values and the calendar year below. The specimen codes, the measured $\delta^{18}O_{shell}$ values, and the calendar years are color-matched. The black dots indicate changes in absolute ages between the specimens used. (For interpretation of the references to color in this figure legend, the reader is referred to the web version of this article.)

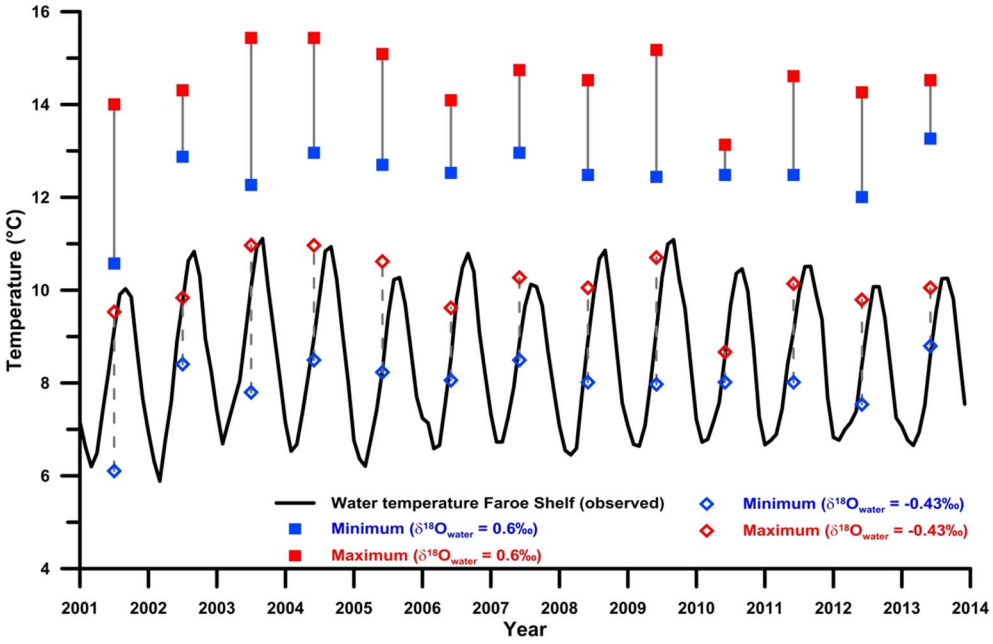

Fig. 6. Reconstructed temperature minima (blue squares and diamonds) and maxima (red squares and diamonds) in relation to the observed temperatures from the coastal station Skopun for the period 2001–2013 using a $\delta^{18}O_{water}$ value of 0.6‰ (squares) and −0.43‰ (diamonds). (For interpretation of the references to color in this figure legend, the reader is referred to the web version of this article.)

the Nordic Seas mixing line (Østbø, 2000) suggest $\delta^{18}O_{water}$ values of approximately 0.25‰ and 0.2‰, respectively. These $\delta^{18}O_{water}$ values would only slightly reduce the offset between reconstructed and observed temperatures. However, the temperature ranges of the instrumental data (approximately 4.0 °C for bottom water temperatures) and the $\delta^{18}O_{shell}$-based reconstructions (approximately 3.5 °C) within a single year/increment are similar. This suggests that the Grossman and Ku (1986) equation seems to produce appropriate temperature ranges based on the $\delta^{18}O_{shell}$ values, meaning that a 1‰ change results in 4.34 °C, but the equation overestimates the absolute values in this region.

Potential causes for the offset could be related to biological effects, the paleotemperature equation used (i.e. Grossman and Ku, 1986) or effects related to the sampling process. An ontogenetic effect seems unlikely because the offset between the observed and reconstructed temperatures is consistent among several specimens and does not vary during different ontogenetic stages (Fig. 5). A constant isotopic disequilibrium during the deposition of the shell carbonate from ambient seawater could explain the offset meaning that a correction factor for the absolute values is required. However, this has not been reported from previous studies (e.g. Schöne et al., 2005c; Schöne et al., 2004; Weidman et al., 1994). Some studies (Aharon, 1991; Gill et al., 1995) have reported that frictional heat during the "dry" drilling process (also used in this study) can alter the $\delta^{18}O$ composition in biogenic aragonite towards lower values. Shifts can be as large as −0.8‰ (Gill et al., 1995) and, in extreme cases, even up to −8‰ (Aharon, 1991). This could explain the exaggerated temperature estimates in our study also in terms of the magnitude. However, the effect of "dry" drilling is rather inconsistent (Aharon, 1991; Gill et al., 1995) and is therefore unlikely to cause a constant offset, as seen in our $\delta^{18}O_{shell}$ record (Fig. 5). In conclusion, the causes for the offset between the reconstructed and observed temperatures remain speculative, and the $\delta^{18}O$ analysis of the shells from the Faroe Shelf has shown that the $\delta^{18}O_{water}$ in the Faroese region needs to be investigated in more detail, but this is beyond the scope of this paper. However, to obtain more data on the $\delta^{18}O$ composition of the waters on the Faroe Shelf, Uni Research, in collaboration with FAMRI, has started systematic sampling and $\delta^{18}O$ analyses of water from this area.

For estimates of the main growing season (defined as the time of the year in which the majority of the formation of the growth increment takes place), we believe that the use of the $\delta^{18}O_{shell}$ values is still legitimate due to the similar ranges of the observed and reconstructed temperatures within a single year/increment. The tendency of the $\delta^{18}O_{shell}$ values being highest in the youngest portion of a growth increment and lowest during the oldest portion of a growth increment (Fig. 5) suggests that the majority of the shell growth occurs somewhere between the seasonal temperature minimum and maximum. On the Faroe Shelf, this usually corresponds to the months of March and September, respectively. Since the temperature difference (~4.0 °C) between these months is similar to what is reconstructed (3–4 °C) for $\delta^{18}O_{shell}$ samples, which represent the youngest and oldest portion of a growth increment, it can be assumed that shell growth occurs over the entire length of this period. However, it is important to mention that the shell growth within the main growing season is not necessarily constant.

4.3. Shell growth variability and instrumental data

A summary of the comparison between the master chronology and phytoplankton is given in Tables 1 and 2, and a visual comparison is provided in Figs. 7, 8, and 9 (a detailed overview of this comparison can be found in Appendix A).

4.3.1. On-shelf phytoplankton

Generally, there is a good agreement between the master chronology and the on-shelf phytoplankton datasets (Fig. 7), and the spatial correlation between the master chronology and the satellite chlorophyll *a* data is strongest in close proximity to the Faroe Islands (Fig. 8).

However, the Pearson correlation between the shell growth and the on-shelf phytoplankton data over or within the time period from 1990 to 2013 is strongly influenced by the relatively large values of the year 2000 and especially in the year 2001 because the Pearson correlation coefficient is generally very sensitive to extreme values and outliers. The Spearman rho correlation coefficient is not affected by extreme values or outliers and is therefore also applied. The Spearman rho correlation between the shell growth and the PP-index and the chlorophyll *a* concentrations is significantly weaker compared to the Pearson correlation. In addition, the Spearman rho correlation between the shell growth and the chlorophyll *a* concentrations does not reach the 95% significance level. However, the extreme values in 2000 and 2001, the

Table 1
Correlation coefficients between the master chronology and various on- and off-shelf phytoplankton datasets. Significant correlations at either a 95% significance level ($p < 0.05$) or a 99% significance level ($p < 0.01$) are indicated.

Shell growth vs. phytoplankton data			
Phytoplankton dataset	Pearson	Spearman's rho	*N*
Chlorophyll *a* Apr–Jun (Skopun)	0.74 ($p < 0.01$)	0.38	17
Primary Production index	0.65 ($p < 0.01$)	0.45 ($p < 0.05$)	24
Fluorescence surface (CTD)			
Feb	− 0.30	− 0.21	12
May	0.19	0.04	17
Sep	0.53 ($p < 0.05$)	0.35	15
Nov	0.06	0.21	14
Fluorescence bottom (CTD)			
Feb	− 0.07	0.01	12
May	0.64 ($p < 0.01$)	0.64 ($p < 0.01$)	17
Sep	0.73 ($p < 0.01$)	0.65 ($p < 0.01$)	15
Nov	0.07	0.23	14
Phytoplankton annual (CPR)	0.40 ($p < 0.01$)	0.50 ($p < 0.01$)	56
Jan	− 0.12	− 0.10	
Feb	− 0.11	− 0.15	
Mar	0.05	− 0.04	
Apr	− 0.03	0.04	
May	0.18	0.16	
Jun	0.16	0.27	
Jul	0.38 ($p < 0.01$)	0.42 ($p < 0.01$)	
Aug	0.30 ($p < 0.05$)	0.43 ($p < 0.01$)	
Sep	0.40 ($p < 0.01$)	0.48 ($p < 0.01$)	
Oct	0.18	0.21	
Nov	0.17	0.34 ($p < 0.05$)	
Dec	0.10	0.22	
PCI annual (CPR)	0.27 ($p < 0.05$)	0.21	

Table 2
Correlation coefficients (Pearson) between the master chronology and water temperatures and air temperatures from the Faroe Shelf. Significant correlations at either a 95% significance level ($p < 0.05$) or a 99% significance level ($p < 0.01$) are indicated. For correlations with water temperatures $N = 77$ and with air temperatures $N = 141$.

Shell growth vs. temperature		
Month	Correlation with water temperature of the Central shelf	Correlation with air temperature of Torshavn
Annual average	− 0.25 ($p < 0.05$)	− 0.06
Jan	− 0.18	− 0.09
Feb	0.05	0.12
Mar	− 0.03	0.12
Apr	− 0.09	0.03
May	− 0.15	− 0.11
Jun	− 0.30 ($p < 0.01$)	− 0.29 ($p < 0.01$)
Jul	− 0.27 ($p < 0.05$)	− 0.25 ($p < 0.01$)
Aug	− 0.34 ($p < 0.01$)	− 0.15
Sep	− 0.33 ($p < 0.01$)	− 0.04
Oct	− 0.20	− 0.05
Nov	− 0.17	0.05
Dec	− 0.19	− 0.02

very low values during the early 1990s, and the overall increasing trend from 1990 to 2001 are present in the phytoplankton-related records as well as in the shell-based record (Fig. 7a).

4.3.2. Off-shelf phytoplankton

Furthermore, there is a significant positive correlation between the shell growth and off-shelf phytoplankton data (CPR) over a longer time scale (Fig. 9), which indicates that the observed patterns from 1990 to 2013 are not just coincidence. Therefore, we believe that there is a strong possibility of a causal relationship between on-shelf and off-shelf phytoplankton dynamics and shell growth.

4.3.3. Temperature

A significant (negative) correlation between the shell growth and water temperatures and air temperatures (Table 2) is found for the summer months. The PP-index and the average June–September water temperatures were selected as predictors of the master chronology in a stepwise multiple regression since these variables are well correlated with the master chronology and provide a good number of data points. For the time period from 1992 to 2013, the adjusted R^2 value for model 1 (master chronology vs PP-index) is 0.33; for model 2 (master chronology vs average June–September water temperatures), 0.16; and for model 3 (master chronology vs PP-index + average June–September water temperatures), 0.39. This shows that the increase in predictive capability of the simple regression of the master chronology and the PP-index only slightly increases when including water temperatures.

5. Discussion

The species *A. islandica* is considered to be a shallow infaunal filter feeder (e.g. Cargnelli et al., 1999) that mainly feeds on phytoplankton and organic detritus (Morton, 2011). In terms of the freshness of the organic matter, specimens of *A. islandica* seem to be highly selective and "feed on the most recent organic matter only" (Erlenkeuser, 1976). In combination with the fact that the Faroe Shelf and the wider Faroese region have been identified as areas in which phytoplankton dynamics are largely reflected in higher trophic levels (Gaard et al., 2002; Hátún et al., 2009), it seems plausible that there could be direct links between primary production and the growth of *A. islandica* in these areas.

The overall good correlations between the shell growth and various on-shelf and off-shelf primary production datasets for the spring and summer months support this hypothesis and are in agreement with the timing of the main growing season (March–September) as determined by the $\delta^{18}O$ analysis and the timing of the main spring bloom (between May and July) on the Faroe Shelf (Hansen et al., 2005). In addition, the spatial correlations between the shell growth and the satellite chlorophyll *a* data are strongest in close proximity to the Faroe Islands, which is in agreement with the locations of the sampling sites. Moreover, the stepwise multiple regression indicates that phytoplankton dynamics are most relevant for the shell growth – more so than temperature.

There are some years (especially after 2002) in which there are no clear positive relationship between the shell growth and on-shelf phytoplankton dynamics (Fig. 7). For example, the high PP-index from 2008 to 2010 does not seem to result in relatively wider growth increments. It is important to remember that the phytoplankton data used for comparison is all near-surface data (except for the CTD fluorescence data), but the shells were collected from deeper water depths of approximately 100 m. Stratification during the summer can occur at the shell locations (Larsen et al., 2009). On the Outer shelf, stratification usually persists after May and until September (Eliasen et al., 2017a). Earlier and more persistent stratification on the Faroe Shelf generally leads to elevated surface phytoplankton concentrations during the initial phase of the spring bloom (May/June) because more phytoplankton is located in the euphotic zone due to a shallower mixed layer depth (Rasmussen et al., 2014). However, more pronounced stratification may also impede the downward flux of phytoplankton so that potential food particles do not reach the bivalves. Moreover, enhanced stratification during the summer months (after the initial phase of the spring bloom) seems to be unfavorable for high phytoplankton concentrations because it hampers a continuous flow of nutrients onto the shelf (Eliasen et al., 2017b). The stratification during the summer months is mainly controlled by the temperature (Eliasen et al., 2017b). Lower summer temperatures usually correspond to a more eroded stratification on the Faroe Shelf, whereas higher summer temperatures have the opposite effect (Eliasen et al., 2017b).

The correlation of the master chronology with the fluorescence data

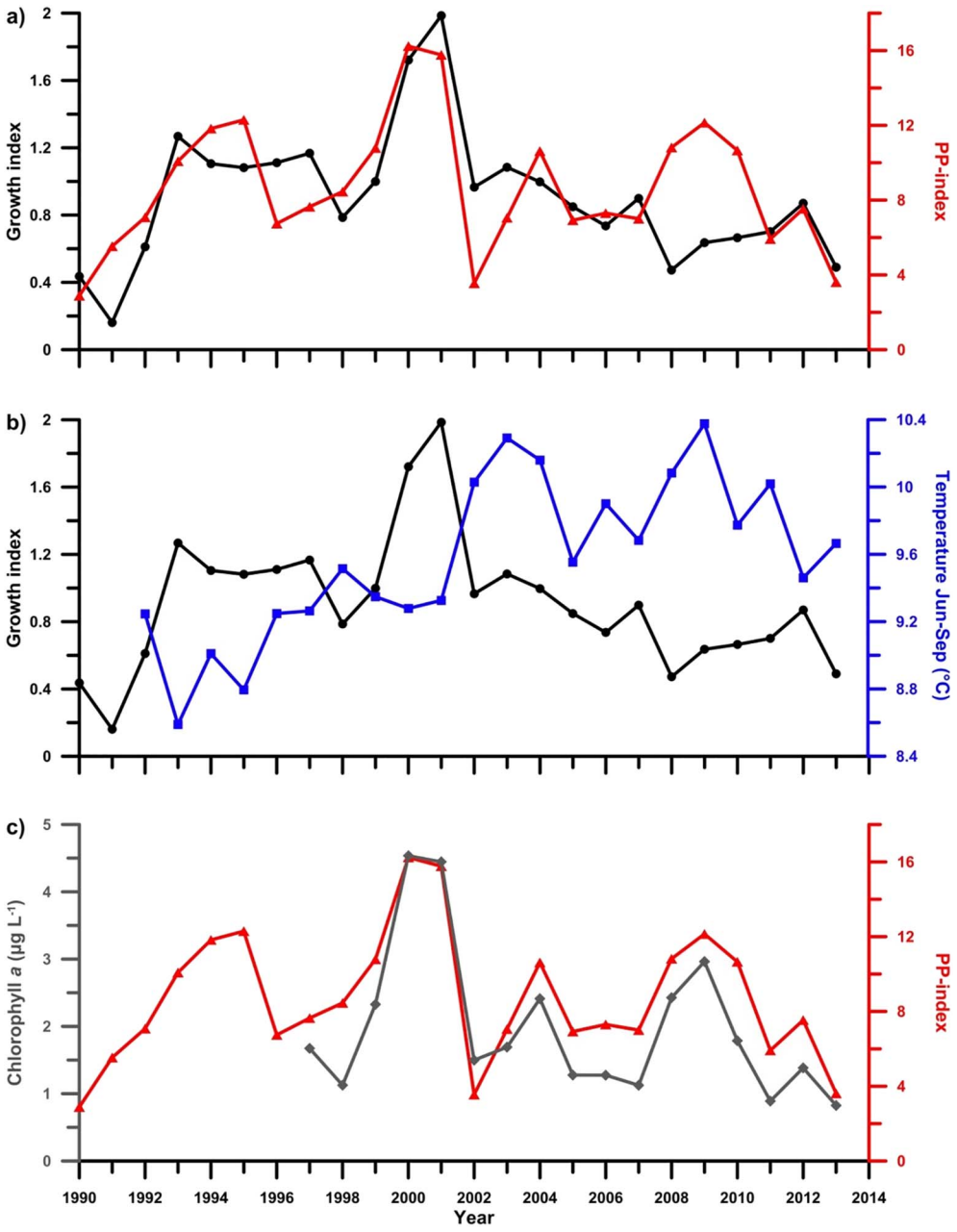

Fig. 7. The growth index of the master chronology (black line & circles) and a) the Primary Production index (PP-index) (red line & triangles) and b) the average June–September on-shelf water temperatures (blue line & squares). c) Integrated April–June chlorophyll *a* concentrations from station S (gray line & diamonds) and the PP-index (red line & triangles). (For interpretation of the references to color in this figure legend, the reader is referred to the web version of this article.)

from the bottom 20 m in the water column is indeed stronger than for the uppermost 30 m. This supports the assumption that stratification has an effect on the shell growth. Additionally, the comparison between the master chronology and the water and air temperatures results in a significant negative correlation mainly for the summer months (Fig. 7b and Table 2). This suggests that the stronger erosion of the summer stratification (more productive conditions on the Central shelf) due to lower summer temperatures is also favorable for the shell growth. A direct influence of temperatures on the shell growth is unlikely because a direct shell growth/temperature relationship is usually positive (Witbaard et al., 1997b), and the inter-annual difference between colder and warmer years (approximately 1–2 °C) relative to the temperature tolerance of *A. islandica* in general is too small. The effect of stratification also explains the discrepancy between the shell growth and the surface phytoplankton concentrations for the years 2008 and 2009 (narrow increments but high surface phytoplankton concentrations) because there is evidence that in 2008 and 2009, stratification began earlier and was more pronounced than in 2002–2007 during the initial phase of the spring bloom (Rasmussen et al., 2014). Thus, a downward flux of potential food particles was presumably impeded during 2008 and 2009. Additionally, the fluorescence profiles from the CTD station E01, for example (Fig. 3), show some evidence that in 2009, the stratification during the summer months was more persistent when compared, for example with the years 2000 and 2001 (extremely wide increments). The years 2000 and 2001 are further characterized by relatively low summer temperatures (favorable phytoplankton conditions), whereas the years 2008 and 2009 (narrow increments) are characterized by relatively high summer temperatures (unfavorable phytoplankton conditions) (Fig. 7b). Another aspect, which is important to mention, is the fact that stratification on the Faroe Shelf can be temporarily interrupted by short-term events such as intense storms, which can occasionally mix up the water column.

In summary, the shell growth in *A. islandica* from the Faroe Shelf is influenced by local on-shelf phytoplankton dynamics but also captures a primary production signal from the wider surroundings of the Faroe Islands. In this regard, local on-shelf effects (strength of the

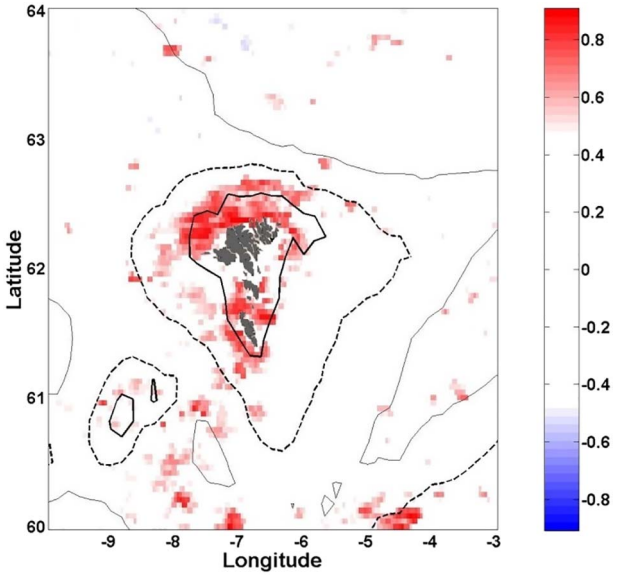

Fig. 8. Spatial correlation (Pearson correlation) between the growth index of the master chronology and the annually averaged satellite chlorophyll *a* measurements from 1998 to 2013. Only correlations at a 95% significance level (or higher) are displayed. The following depth contours are displayed: 100 m (thick black), 300 m (dashed) and 1000 m (thin). (For interpretation of the references to color in this figure legend, the reader is referred to the web version of this article.)

stratification during the initial phase of the spring bloom, erosion of the summer stratification due to lower summer temperatures, possible temporary breakdowns of the summer stratification due to storms) seem to serve as an inter-annual amplifier and/or inhibitor on top of decadal fluctuations of phytoplankton concentrations in the wider Faroese region. For the years 2000 and 2001, for example, favorable conditions for rapid shell growth (well-mixed water column on the Faroe Shelf during the summer, earlier spring bloom) could have resulted in extraordinary wide growth increments, although the wider Faroese region did not experience phytoplankton concentrations higher than normal. Similarly, the years 1993 and 1994 correspond to relatively wide growth increments despite the generally low phytoplankton concentrations in the wider region.

6. Conclusions

The findings of our study suggest that phytoplankton dynamics on the Faroe Shelf and in the wider Faroese region are recorded in the shell growth variability of *A. islandica* shells from the Faroe Shelf. This is especially true at lower (decadal) frequencies and during extreme years with either extraordinary high or low phytoplankton concentrations. Local dynamics such as stratification intensity and persistency and the potential temporary mixing of the water column due to short-term events can either amplify or inhibit the off-shelf phytoplankton signal in the shells on inter-annual timescales. Thus, the shell growth variability can serve as a tool to identify times of large inter-annual changes in the phytoplankton concentration on the Faroe Shelf. In contrast, longer periods of consistently relatively narrow or wide growth increments should be more attributed to phytoplankton dynamics in a broader geographical context. The analysis of the $\delta^{18}O_{shell}$ clearly shows a seasonal temperature signal, and the $\delta^{18}O_{shell}$-based reconstructed temperature ranges in single growth increments allow a fairly precise estimation of the main growing season. However, the absolute values of reconstructed and observed water temperatures show a consistent offset — a finding that needs a more detailed investigation in future studies.

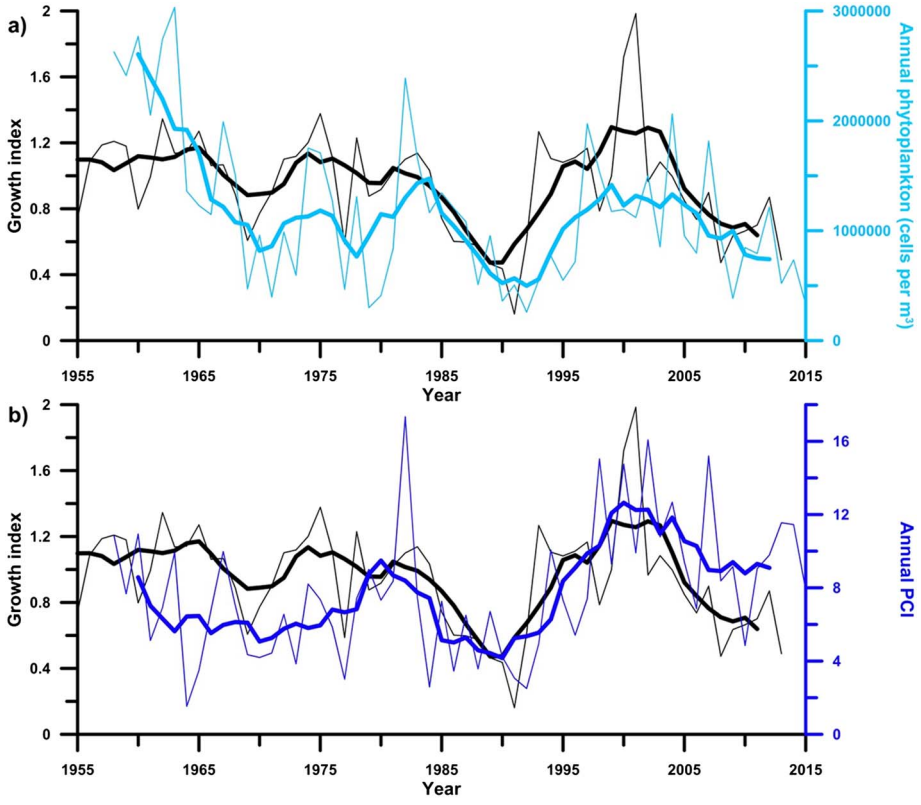

Fig. 9. Growth index of the master chronology (black line) and (a) the total annual phytoplankton concentrations in the CPR standard area B4 (light blue line) and (b) the annual Phytoplankton Color Index (PCI) from the CPR standard area B4 (blue line). Thick lines are the 6-year running means of the respective variables. (For interpretation of the references to color in this figure legend, the reader is referred to the web version of this article.)

Acknowledgements

This work is a result of the EU-funded ITN ARAMACC (604802) project and the Norwegian Research Council-funded project ECHO (240555) as well as contributions from the Bjerknes Centre for Climate Research (129000), the Meltzer Research Fund (7188), and PhD student support from the Norwegian Research School in Climate Dynamics (ResClim). Special recognition goes to the Faroe Marine Research Institute FAMRI, which provided a large part of the instrumental data. In particular, we want to thank the FAMRI researchers Karin M. H. Larsen, Una Matras, Petur Steingrund, Sólvá Káradóttir Eliasen and Bogi Hansen for their constructive input and feedback during the process of this work. Furthermore, we want to thank Bernd Schöne from the Institute of Geoscience at the Johannes Gutenberg University in Mainz, Germany for his input on the outcome regarding the geochemical analysis of our samples. Last, we want to thank two anonymous reviewers for helping us improve the manuscript.

Appendix A

Table A1
Pearson correlation coefficients between the single time series and the master series in 30-year segments lagged by 15 years.

Time series	Life span	1635–1664	1650–1679	1665–1694	1680–1709	1695–1724
MH36-47D	1646–1868	0.77	0.78	0.73	0.81	0.76
MH36-90S	1674–1913			0.67	0.70	0.77
MH36-91S	1685–1938				0.81	0.81
MH36-92S	1648–1853	0.75	0.79	0.83	0.91	0.79
MH36-93S	1647–1886	0.75	0.76	0.79	0.85	0.77
MH39-7AS	1700–2003					0.74
MH40-34S	1625–1846	0.42	0.59	0.63	0.83	0.86
Average segment correlation		0.67	0.73	0.73	0.82	0.79
Time series	Life span	1710–1739	1725–1754	1740–1769	1755–1784	1770–1799
MH36-47D	1646–1868	0.70	0.58	0.68	0.67	0.70
MH36-90S	1674–1913	0.84	0.90	0.88	0.75	0.72
MH36-91S	1685–1938	0.68	0.70	0.89	0.86	0.70
MH36-92S	1648–1853	0.60	0.64	0.85	0.83	0.78
MH36-93S	1647–1886	0.71	0.69	0.64	0.6	0.76
MH39-7AS	1700–2003	0.66	0.62	0.66	0.74	0.82
MH39-8AS	1718–2011	0.80	0.75	0.84	0.72	0.39
MH40-34S	1625–1846	0.75	0.66	0.53	0.58	0.82
MH40-35S	1732–1994		0.68	0.63	0.85	0.88
MH40-36D	1726–2008		0.77	0.84	0.88	0.84
Average segment correlation		0.72	0.7	0.74	0.75	0.74
Time series	Life span	1785–1814	1800–1829	1815–1844	1830–1859	1845–1874
GS14/4-12AS	1793–1934	0.84	0.88	0.90	0.78	0.79
GS14/4-7AS	1831–2011				0.77	0.75
MH36-47D	1646–1868	0.78	0.75	0.86	0.82	0.76
MH36-90S	1674–1913	0.82	0.82	0.89	0.74	0.70
MH36-91S	1685–1938	0.60	0.69	0.85	0.70	0.51
MH36-92S	1648–1853	0.84	0.89	0.85	0.79	
MH36-93S	1647–1886	0.92	0.79	0.79	0.66	0.59
MH39-10AS	1825–2003			0.80	0.80	0.78
MH39-21S	1804–1989		0.53	0.86[a]	0.76	0.76
MH39-7AS	1700–2003	0.88	0.91	0.88	0.78	0.74
MH39-8AS	1718–2011	0.51	0.75[a]	0.90	0.84	0.80
MH40-20AS	1813–2004		0.74	0.80	0.85	0.79
MH40-23S	1816–2004			0.78	0.68	0.61
MH40-24S	1851–1990					0.87
MH40-26S	1850–1969					0.80
MH40-27S	1825–2006			0.81	0.85	0.84
MH40-28S	1851–1976					0.79
MH40-33D	1849–2000					0.81
MH40-34S	1625–1846	0.78	0.77	0.74	0.73	
MH40-35S	1732–1994	0.90	0.92	0.95	0.87	0.78
MH40-36D	1726–2008	0.79	0.83	0.94	0.90	0.84
MH40-37D	1830–1999				0.84	0.74
MH40-38D	1831–2006				0.83	0.89
MH40-39D	1816–1895			0.82	0.70	0.56
Average segment correlation		0.79	0.79	0.85	0.78	0.75
Time series	Life span	1860–1889	1875–1904	1890–1919	1905–1934	1920–1949

GS14/23-47LS	1909–013				0.61	0.33
GS14/24-87LS	1926–2013					0.36[a]
GS14/4-12AS	1793–1934	0.94	0.93	0.90	0.90	
GS14/4-7AS	1831–2011	0.84	0.82	0.85	0.90	0.80
MH36-90S	1674–1913	0.87	0.85	0.77		
MH36-91S	1685–1938	0.80	0.85	0.83	0.81	0.81
MH36-93S	1647–1886	0.79				
MH39-10AS	1825–2003	0.90	0.90	0.82	0.76	0.77
MH39-21S	1804–1989	0.92	0.92	0.87	0.89	0.81
MH39-7AS	1700–2003	0.78	0.77	0.85	0.90	0.79
MH39-8AS	1718–2011	0.88	0.93	0.90	0.83	0.75
MH40-20AS	1813–2004	0.92	0.91	0.88	0.91	0.91
MH40-23S	1816–2004	0.84	0.89	0.92	0.92	0.76
MH40-24S	1851–1990	0.87	0.90	0.88	0.86	0.86
MH40-26S	1850–1969	0.87	0.94	0.93	0.88	0.82
MH40-27S	1825–2006	0.93	0.92	0.94	0.93	0.85
MH40-28S	1851–1976	0.85	0.86	0.83	0.88	0.82
MH40-33D	1849–2000	0.88	0.88	0.93	0.96	0.83
MH40-35S	1732–1994	0.80	0.85	0.94	0.86	0.64
MH40-36D	1726–2008	0.81	0.82	0.93	0.93	0.89
MH40-37D	1830–1999	0.88	0.96	0.94	0.89	0.85
MH40-38D	1831–2006	0.96	0.92	0.91	0.88	0.83
MH40-39D	1816–1895	0.62	0.62			
Average segment correlation		0.85	0.87	0.89	0.87	0.76

Time series	Life span	1935–1964	1950–1979	1965–1994	1980–2009	1995–2024
GS14/13-38AS	1967–2012			0.72	0.84	0.85
GS14/13-6LS	1985–2013				0.82	
GS14/13-7LS	1954–2013		0.81	0.79	0.84	0.83
GS14/14-5LD	1966–2013			0.86	0.91	0.91
GS14/14-7LD	1966–2013			0.81	0.89	0.92
GS14/23-41LS	1972–2013			0.39	0.16	0.14
GS14/23-47LS	1909–2013	0.04	0.42[a]	0.75	0.81	0.67
GS14/23-49LS	1961–2013		0.58	0.67	0.61	0.54
GS14/24-84LS	1954–2013		0.59	0.73	0.74	0.73
GS14/24-87LS	1926–2013	0.29	0.44	0.68	0.69	0.65
GS14/4-7AS	1831–2011	0.64	0.63	0.74	0.75	0.72
MH37-10AS	1960–2006		0.63	0.71	0.86	
MH38-13AS	1936–2012	0.74	0.54	0.47	0.85	0.86
MH38-1AS	1959–2009		0.69	0.71	0.92	
MH38-2AS	1964–2010		0.82	0.82	0.89	0.90
MH38-3AS	1973–2012			0.77	0.78	0.80
MH39-10AS	1825–2003	0.70	0.69	0.83	0.84	
MH39-21S	1804–1989	0.67	0.54	0.55		
MH39-7AS	1700–2003	0.56	0.63	0.80	0.80	
MH39-8AS	1718–2011	0.78	0.79	0.84	0.86	0.83
MH40-20AS	1813–2004	0.92	0.81	0.76	0.84	
MH40-23S	1816–2004	0.73	0.91	0.86	0.88	
MH40-24S	1851–1990	0.86	0.88	0.88		
MH40-26S	1850–1969	0.77	0.75			
MH40-27S	1825–2006	0.83	0.88	0.86	0.74	
MH40-28S	1851–1976	0.70	0.73			
MH40-33D	1849–2000	0.79	0.81	0.81	0.80	
MH40-35S	1732–1994	0.54	0.68	0.67		
MH40-36D	1726–2008	0.86	0.86	0.87	0.82	
MH40-37D	1830–1999	0.81	0.76	0.80	0.77	
MH40-38D	1831–2006	0.86	0.81	0.80	0.77	
Average segment correlation		0.69	0.71	0.75	0.79	0.74

[a] Correlation higher at other than dated position.

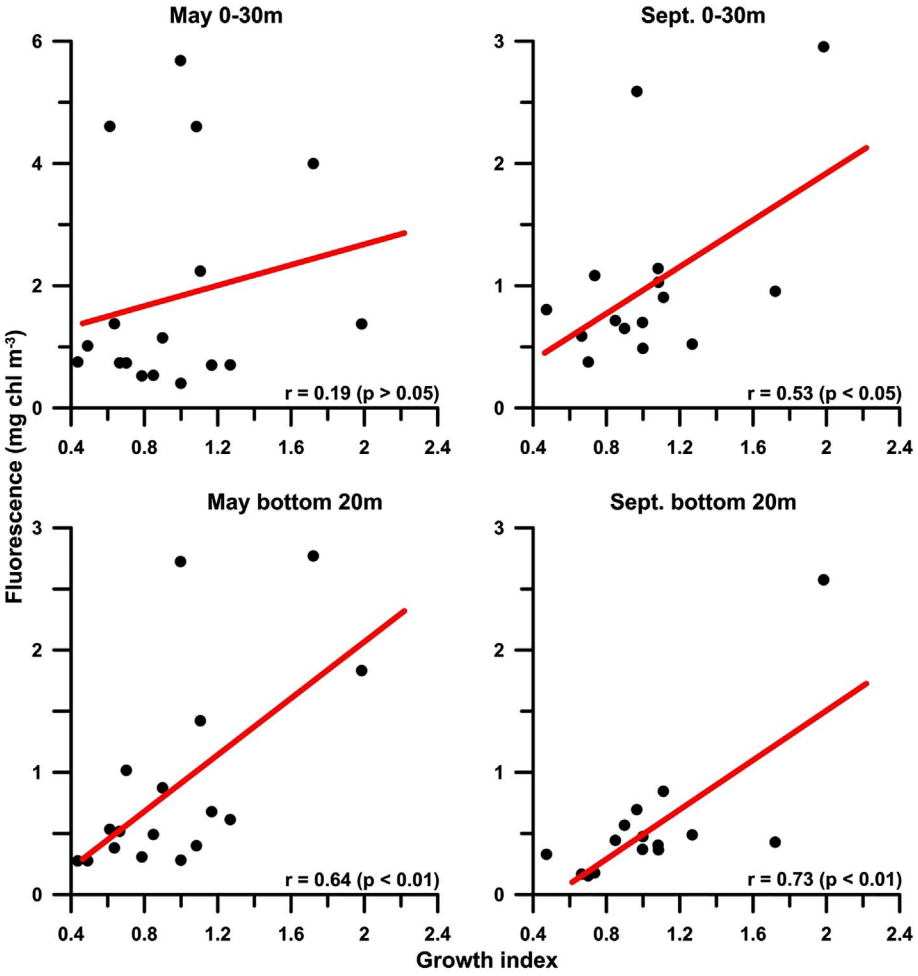

Fig. A1. Cross-plots of the surface (top) and bottom (bottom) fluorescence values for the months May and September and the growth index of the master chronology. The fluorescence values are derived from the CTD station E01. The red lines represent the linear regression lines.

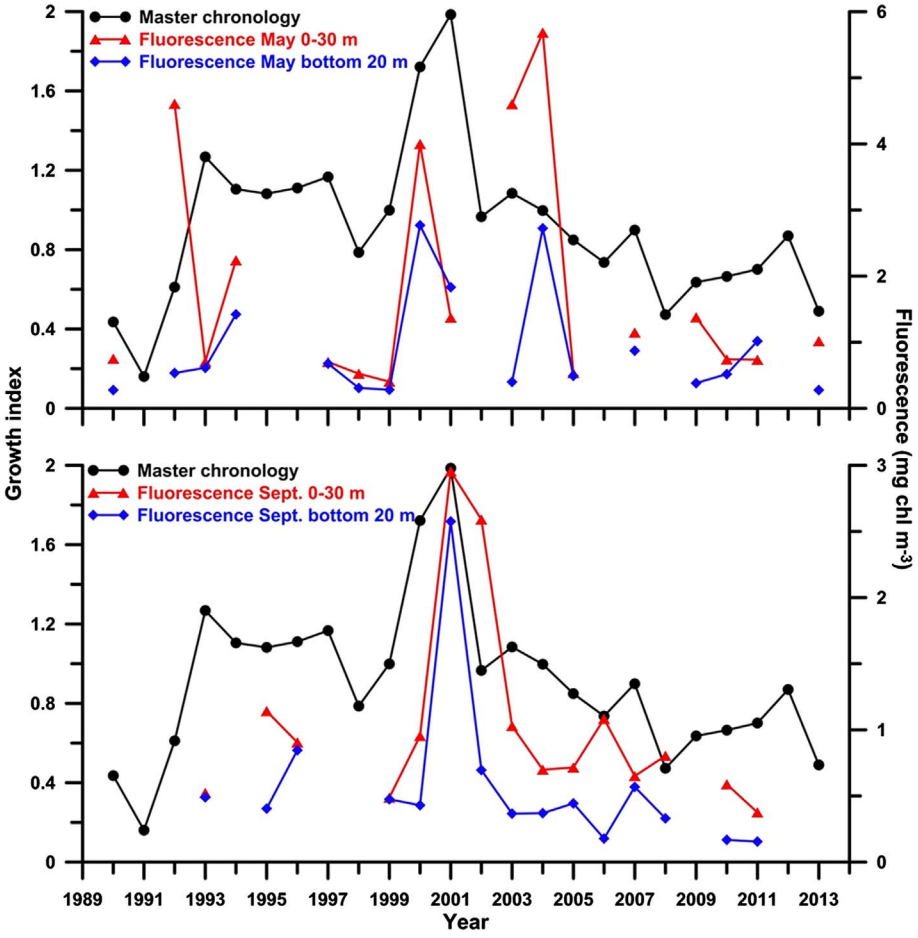

Fig. A2. Growth index of the master chronology (black line & black circles) in comparison with the surface (red line & red triangles) and bottom fluorescence (blue line & blue diamonds) values from the CTD station E01 for the months May (top) and September (bottom).

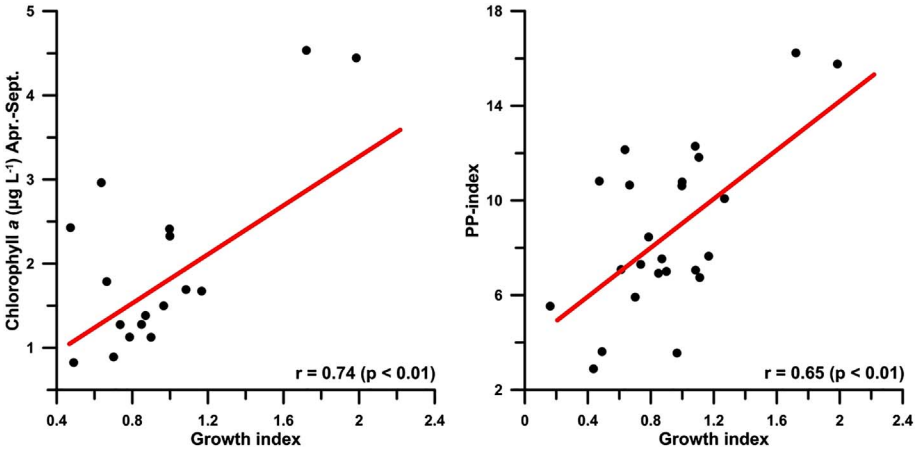

Fig. A3. Cross-plots of the growth index of the master chronology and the average chlorophyll *a* concentrations from April–September (left) and the Primary Production index (PP-index) (right). The red lines represent the linear regression lines.

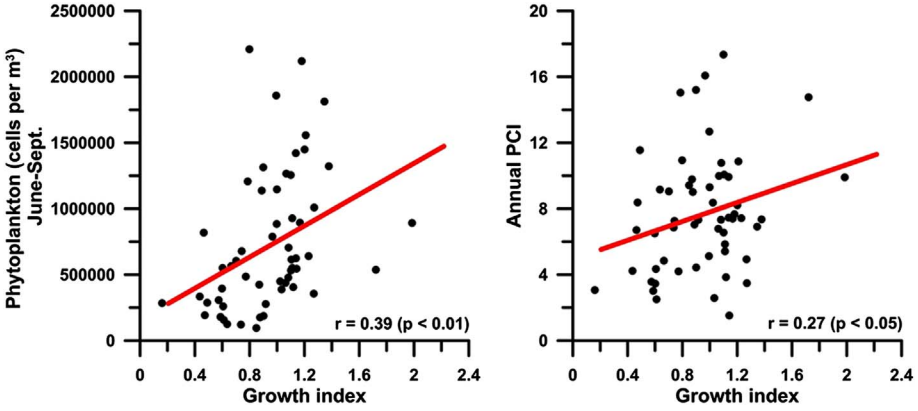

Fig. A4. Cross-plots of the growth index of the master chronology and phytoplankton metrics from the Continuous Plankton Recorder (CPR) standard area B4. Left: total phytoplankton concentration (June–September); right: the annual Phytoplankton Color Index (PCI). The red lines represent the linear regression lines.

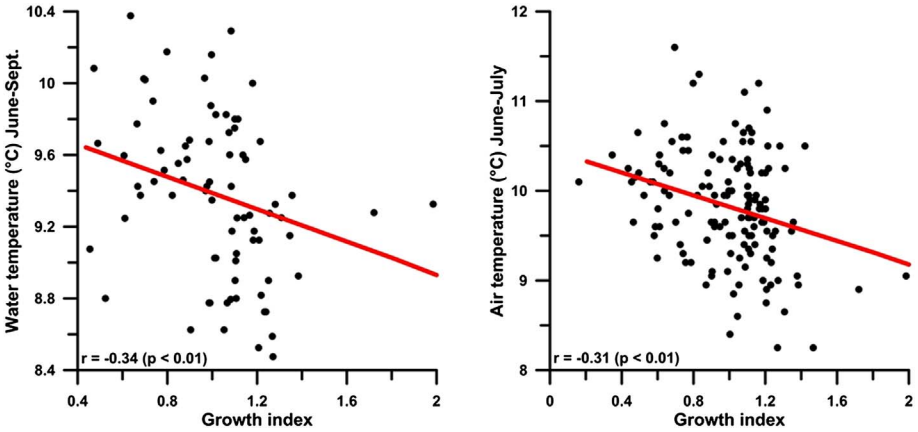

Fig. A5. Cross-plots of the growth index of the master chronology and the average water temperatures on the Central shelf from June–September (left) and the average air temperatures in Torshavn from June–July (right). The red lines represent the linear regression lines.

References

Aharon, P., 1991. Recorders of reef environment histories - stable isotopes in corals, giant clams, and calcareous algae. Coral Reefs 10, 71–90.

Baillie, M.G.L., 1982. Tree-ring Dating and Archaeology. University of Chicago Press.

Ballesta-Artero, I., Witbaard, R., Carroll, M.L., van der Meer, J., 2017. Environmental factors regulating gaping activity of the bivalve *Arctica islandica* in Northern Norway. Mar. Biol. 164, 116.

Batten, S.D., Clark, R., Flinkman, J., Hays, G.C., John, E., John, A.W.G., Jonas, T., Lindley, J.A., Stevens, D.P., Walne, A., 2003. CPR sampling: the technical background, materials and methods, consistency and comparability. Prog. Oceanogr. 58, 193–215.

Butler, P.G., Richardson, C.A., Scourse, J.D., Witbaard, R., Schöne, B.R., Fraser, N.M., Wanamaker Jr., A.D., Bryant, C.L., Harris, I., Robertson, I., 2009a. Accurate increment identification and the spatial extent of the common signal in five *Arctica islandica* chronologies from the Fladen Ground, northern North Sea. Paleoceanography 24, PA2210.

Butler, P.G., Scourse, J.D., Richardson, C.A., Wanamaker Jr, A.D., Bryant, C.L., Bennell, J.D., 2009b. Continuous marine radiocarbon reservoir calibration and the 13C Suess effect in the Irish Sea: results from the first multi-centennial shell-based marine master chronology. Earth Planet. Sci. Lett. 279, 230–241.

Butler, P.G., Richardson, C.A., Scourse, J.D., Wanamaker Jr, A.D., Shammon, T.M., Bennell, J.D., 2010. Marine climate in the Irish Sea: analysis of a 489-year marine master chronology derived from growth increments in the shell of the clam Arctica Islandica. Quat. Sci. Rev. 29, 1614–1632.

Butler, P.G., Wanamaker Jr, A.D., Scourse, J.D., Richardson, C.A., Reynolds, D.J., 2011. Long-term stability of δ13C with respect to biological age in the aragonite shell of mature specimens of the bivalve mollusk *Arctica islandica*. Palaeogeogr. Palaeoclimatol. Palaeoecol. 302, 21–30.

Butler, P.G., Wanamaker Jr., A.D., Scourse, J.D., Richardson, C.A., Reynolds, D.J., 2013. Variability of marine climate on the North Icelandic Shelf in a 1357-year proxy archive based on growth increments in the bivalve *Arctica islandica*. Palaeogeogr. Palaeoclimatol. Palaeoecol. 373, 141–151.

Cargnelli, L.M., Griesbach, S.L., Packer, D.B., Weissberger, E., 1999. Ocean quahog, *Arctica islandica*, life history and habitat characteristics NOAA. In: Technical Memorandum NMFS-NE-148, pp. 1–12.

Cook, E.R., Holmes, R.L., 1986. Users Manual for Program ARSTAN. Laboratory of Tree-Ring Research, University of Arizona, Tuscon, U.S.A.

Craig, H., Gordon, L.I., 1965. Deuterium and oxygen-18 variations in the ocean and marine atmosphere. In: Spoleto Conference Proceedings, Cons. Naz. Ric., V. Lischi Figli.

Debes, H.H., Gaard, E., Hansen, B., 2008. Primary production on the Faroe shelf: temporal variability and environmental influence. J. Mar. Syst. 74, 686–697.

Dunca, E., Mutvei, H., Goransson, P., Morth, C.M., Schöne, B.R., Whitehouse, M.J., Elfman, M., Baden, S.P., 2009. Using ocean quahog (*Arctica islandica*) shells to reconstruct palaeoenvironment in Öresund, Kattegat and Skagerrak, Sweden. Int. J. Earth Sci. 98, 3–17.

Eliasen, S.K., Gaard, E., Hansen, B., Larsen, K.M.H., 2005. A "horizontal Sverdrup mechanism" may control the spring bloom around small oceanic islands and over banks. J. Mar. Syst. 56, 352–362.

Eliasen, K., Reinert, J., Gaard, E., Hansen, B., Jacobsen, J.A., Gronkjaer, P., Christensen, J.T., 2011. Sandeel as a link between primary production and higher trophic levels on the Faroe shelf. Mar. Ecol. Prog. Ser. 438, 185–194.

Eliasen, S.K., Hansen, B., Larsen, K.M.H., Hátún, H., 2016. The exchange of water between the Faroe Shelf and the surrounding waters and its effect on the primary production. J. Mar. Syst. 153, 1–9.

Eliasen, S.K., Hátún, H., Larsen, K.M.H., Hansen, B., Rasmussen, T.A.S., 2017a. Phenologically distinct phytoplankton regions on the Faroe Shelf - identified by satellite data, in-situ observations and model. J. Mar. Syst. 169, 99–110.

Eliasen, S.K., Hátún, H., Larsen, K.M.H., Jacobsen, S., 2017b. Faroe shelf bloom phenology - the importance of ocean-to-shelf silicate fluxes. Cont. Shelf Res. 143, 43–53.

Erlenkeuser, H., 1976. 14C and 13C isotope concentration in modern marine mussels from sedimentary habitats. Naturwissenschaften 63, 338.

Gaard, E., 2003. Plankton variability on the Faroe Shelf during the 1990s. ICES Mar. Sci. Symp. 219, 182–189.

Gaard, E., Hansen, B., Heinesen, S.P., 1998. Phytoplankton variability on the Faroe Shelf. ICES J. Mar. Sci. 55, 688–696.

Gaard, E., Hansen, B., Olsen, B., Reinert, J., 2002. Ecological features and recent trends in the physical environment, plankton, fish stocks, and seabirds in the Faroe Shelf ecosystem. In: Sherman, K., Skjoldal, H.-R. (Eds.), Large Marine Ecosystems of the North Atlantic. Elsiever, London, pp. 245–265.

Gill, I., Olson, J.J., Hubbard, D.K., 1995. Corals, paleotemperature records, and the

aragonite-calcite transformation. Geology 23, 333–336.
Grossman, E.L., Ku, T.L., 1986. Oxygen and carbon isotope fractionation in biogenic aragonite - temperature effects. Chem. Geol. 59, 59–74.
Hansen, B., 1992. Residual and tidal currents on the Faroe plateau. In: ICES CM1992/C:12, unpublished.
Hansen, B., Østerhus, S., 2000. North Atlantic–Nordic Seas exchanges. Prog. Oceanogr. 45, 109–208.
Hansen, B., Østerhus, S., Hatun, H., Kristiansen, R., Larsen, K.M.H., 2003. The Iceland-Faroe inflow of Atlantic water to the Nordic Seas. Prog. Oceanogr. 59, 443–474.
Hansen, B., Eliasen, S.K., Gaard, E., Larsen, K.M.H., 2005. Climatic effects on plankton and productivity on the Faroe Shelf. ICES J. Mar. Sci. 62, 1224–1232.
Hátún, H., Payne, M.R., Beaugrand, G., Reid, P.C., Sandø, A.B., Drange, H., Hansen, B., Jacobsen, J.A., Bloch, D., 2009. Large bio-geographical shifts in the north-eastern Atlantic Ocean: from the subpolar gyre, via plankton, to blue whiting and pilot whales. Prog. Oceanogr. 80, 149–162.
Homrum, E.I., Hansen, B., Steingrund, P., Hátún, H., 2012. Growth, maturation, diet and distribution of saithe (*Pollachius virens*) in Faroese waters (NE Atlantic). Mar. Biol. Res. 8, 246–254.
Jones, D.S., 1980. Annual cycle of shell growth increment formation in two continental shelf bivalves and its paleoecologic significance. Paleobiology 6, 331–340.
Larsen, K.M.H., 2003. An Investigation of the Faroe Shelf Front. Master thesis. Geophysical Institute, University of Bergen, Bergen, Norway.
Larsen, K.M.H., Hansen, B., Svendsen, H., 2008. Faroe Shelf water. Cont. Shelf Res. 28, 1754–1768.
Larsen, K.M.H., Hansen, B., Svendsen, H., 2009. The Faroe Shelf front: properties and exchange. J. Mar. Syst. 78, 9–17.
Larsen, K.M.H., Hansen, B., Mortensen, E., Kristiansen, R., 2012. Faroese standard sections 1988–2010. In: Larsen, K.M.H., Hansen, B., Mortensen, E., Kristiansen, R. (Eds.), Havstovan Nr.: 12-02 - Technical Report. Havstovan, Torshavn, Faroe Islands, pp. 1–38.
Linnaeus, C., 1767. Systema naturae sive regna tria naturae, secundum classes, ordines, genera, species, cum characteribus, differentiis, synonymis, locis, Tomus 1, Pars 212th ed. Laurentii Salvii, Holmiae, pp. 533–1327.
Mann, R., 1989. Larval ecology of *Arctica islandica* on the inner continental shelf of the eastern United States. J. Shellfish Res. 8, 464.
Marali, S., Schöne, B.R., 2015. Oceanographic control on shell growth of *Arctica islandica* (Bivalvia) in surface waters of Northeast Iceland - implications for paleoclimate reconstructions. Palaeogeogr. Palaeoclimatol. Palaeoecol. 420, 138–149.
Marchitto, T.M., Jones, G.A., Goodfriend, G.A., Weidman, C.R., 2000. Precise temporal correlation of holocene mollusk shells using sclerochronology. Quat. Res. 53, 236–246.
Maritorena, S., Siegel, D.A., Peterson, A.R., 2002. Optimization of a semianalytical ocean color model for global-scale applications. Appl. Opt. 41, 2705–2714.
Mette, M.J., Wanamaker Jr, A.D., Carroll, M.L., Ambrose Jr, W.G., Retelle, M.J., 2016. Linking large-scale climate variability with *Arctica islandica* shell growth and geochemistry in northern Norway. Limnol. Oceanogr. 61, 748–764.
Morton, B., 2011. The biology and functional morphology of *Arctica islandica* (Bivalvia: Arcticidae): a gerontophilic living fossil. Mar. Biol. Res. 7, 540–553.
Nicol, J., 1951. Recent species of the veneroid pelecypod Arctica. J. Wash. Acad. Sci. 41, 102–106.
Østbø, M., 2000. Oxygen isotope characteristics of water masses and mixing in the Nordic Seas. PhD thesis. Faculty of Physics, Informatic and Mathemathis. Norwegian University of Science and Technology, Trondheim, Norway.
Rasmussen, T.A.S., Olsen, S.M., Hansen, B., Hátún, H., Larsen, K.M.H., 2014. The Faroe shelf circulation and its potential impact on the primary production. Cont. Shelf Res. 88, 171–184.
Reynolds, D.J., Scourse, J.D., Halloran, P.R., Nederbragt, A.J., Wanamaker, A.D., Butler, P.G., Richardson, C.A., Heinemeier, J., Eiriksson, J., Knudsen, K.L., Hall, I.R., 2016. Annually resolved North Atlantic marine climate over the last millennium. Nat. Commun. 7, 13502.
Schöne, B.R., 2013. *Arctica islandica* (Bivalvia): a unique paleoenvironmental archive of the northern North Atlantic Ocean. Glob. Planet. Chang. 111, 199–225.
Schöne, B.R., Castro, A.D.F., Fiebig, J., Houk, S.D., Oschmann, W., Kröncke, I., 2004. Sea surface water temperatures over the period 1884-1983 reconstructed from oxygen isotope ratios of a bivalve mollusk shell (Arctica islandica, southern North Sea). Palaeogeogr. Palaeoclimatol. Palaeoecol. 212, 215–232.
Schöne, B.R., Houk, S.D., Freyre Castro, A.D., Fiebig, J., Kröncke, I., Dreyer, W., Oschmann, W., 2005a. Daily growth rates in shells of *Arctica islandica*: assessing subseasonal environmental controls on a long-lived bivalve mollusk. PALAIOS 20, 78–92.
Schöne, B.R., Pfeiffer, M., Gleß, R., Hickson, J., Johnson, A.L.A., Dreyer, W., Oschmann, W., 2005b. Climate records from a bivalved Methuselah (*Arctica islandica*, Mollusca; Iceland). Palaeogeogr. Palaeoclimatol. Palaeoecol. 228, 130–148.
Schöne, B.R., Pfeiffer, M., Pohlmann, T., Siegismund, F., 2005c. A seasonally resolved bottom-water temperature record for the period ad 1866–2002 based on shells of *Arctica islandica* (Mollusca, North Sea). Int. J. Climatol. 25, 947–962.
Schöne, B.R., Zhang, Z.J., Radermacher, P., Thebault, J., Jacob, D.E., Nunn, E.V., Maurer, A.F., 2011. Sr/Ca and Mg/Ca ratios of ontogenetically old, long-lived bivalve shells (*Arctica islandica*) and their function as paleotemperature proxies. Palaeogeogr. Palaeoclimatol. Palaeoecol. 302, 52–64.
Scourse, J.D., Richardson, C.A., Forsythe, G., Harris, I., Heinemeier, J., Fraser, N., Briffa, K.R., Jones, P., 2006. First cross-matched floating chronology from the marine fossil record: data from growth lines of the long-lived bivalve mollusc *Arctica islandica*. The Holocene 16, 967–974.
Scourse, J.D., Wanamaker, A.D., Weidman, C.R., Heinemeier, J., Reimer, P.J., Butler, P.G., Witbaard, R., Richardson, C.A., 2012. The marine radiocarbon bomb pulse across the temperate North Atlantic: a compilation of Δ14C time histories from *Arctica islandica* growth increments. Radiocarbon 54, 165–186.
Sharp, Z., 2007. Principles of Stable Isotope Geochemistry, 1st edition. Pearson, Upper Saddle River, N.J.
Speer, J.H., 2010. Fundamentals of Tree Ring Research. The Univeristy of Arizona Press, Tuscon, Arizona.
Steingrund, P., Gaard, E., 2005. Relationship between phytoplankton production and cod production on the Faroe shelf. ICES J. Mar. Sci. 62, 163–176.
Wanamaker Jr., A.D., Hetzinger, S., Halfar, J., 2011. Reconstructing mid- to high-latitude marine climate and ocean variability using bivalves, coralline algae, and marine sediment cores from the Northern Hemisphere. Palaeogeogr. Palaeoclimatol. Palaeoecol. 302, 1–9.
Weidman, C.R., Jones, G.A., 1993. A shell-derived time history of bomb 14C on Georges Bank and its Labrador Sea implication. J. Geophys. Res. 98, 14577–14588.
Weidman, C.R., Jones, G.H., Lohmann, K.C., 1994. The long-lived mollusc *Arctica islandica*: a new paleoceanographic tool for the reconstruction of bottom temperatures for the continental shelves of the northern North Atlantic Ocean. J. Geophys. Res. Oceans 99, 18305–18314.
Wigley, T.M.L., Briffa, K.R., Jones, P.D., 1984. On the average value of correlated time-series, with applications in dendroclimatology and hydrometeorology. J. Clim. Appl. Meteorol. 23, 201–213.
Witbaard, R., Duineveld, G.C.A., J., d.W.P.A.W., 1997a. A long-term growth record derived from *Arctica islandica* (Mollusca, Bivalvia) from the Fladen Ground (northern North Sea). J. Mar. Biol. Assoc. U. K. 77, 801–816.
Witbaard, R., Franken, R., Visser, B., 1997b. Growth of juvenile *Arctica islandica* under experimental conditions. Helgoländer Meeresun. 51, 417–431.